The carrier concentration dependence of weak-localisation parameters in bismuth-based systems

1990 J. Phys.: Condens. Matter 2 3529

(http://iopscience.iop.org/0953-8984/2/15/009)

J. Phys.: Condens. Matter **2** (1990) 3529–3538. Printed in the UK

The carrier concentration dependence of weak-localisation parameters in bismuth-based systems

H White and D S McLachlan

Department of Physics and Condensed Matter Research Group, University of the Witwatersrand, Wits 2050, South Africa

Received 5 September 1989

Abstract. The effect of varying the carrier concentration and type (electrons and holes, or holes only) on weak-antilocalisation parameters such as the inelastic scattering length is studied. Disordered bismuth-based films are used, and the carrier concentration and type are changed by doping with tin. Two methods of doping are utilised. In the first, the films are sputtered from alloyed bismuth–tin targets. The second method involved interleaving bismuth layers 4.0 nm thick with tin layers less than a monolayer thick. It is shown that the sign of the temperature coefficient of resistance results from the delicate interplay between the weak antilocalisation and associated electron–electron interaction channels. It is also shown that the inelastic scattering length is only weakly dependent on carrier concentration but strongly dependent on film thickness.

1. Introduction

The theories of weak localisation (WL) and weak antilocalisation (WAL) have led to a deeper understanding of electronic transport processes in disordered metallic systems. After the development of the universal single-parameter conductance scaling function by Abrahams *et al* (1979), Gorkov *et al* (1979) showed that non-trivial phase interference effects become increasingly important as the disorder within a metallic system is increased. In particular, Gorkov *et al* (1979) showed that phase interference processes give rise to a logarithmic resistance correction (in temperature) in two-dimensional (2D) systems. The magnetic field dependence of the conductivity in the WL regime was calculated by Hikami *et al* (1980), who in the same paper also calculated the effects of spin–orbit coupling and magnetic impurities. As the correction to the conductivity in the presence of strong spin–orbit coupling is negative (as opposed to positive in the absence of spin–orbit scattering), WL in the presence of strong spin–orbit scattering is known as weak antilocalisation (WAL). Bergmann (1983) pointed out that the magnetoresistance theories of WL and WAL provide a probe of parameters such as the inelastic, elastic and spin–orbit scattering times. This is accomplished by 'fitting' the theories to experimental magnetoresistance data and, as the variable parameters contained in the magnetoresistance theories include the scattering times, these parameters can be determined.

Generally, in the WAL regime, the temperature T dependence of the inelastic scattering length L_{in} (related to the inelastic scattering time τ_{in} by $L_{in} = (D\tau_{in})^{1/2}$) where D is the diffusion constant) is given by

$$L_{in}(T) = L_{in}(1\text{ K})/T^{p/2}. \tag{1}$$

Values of $p/2$ of 0.5, 0.75 and 1 have been predicted theoretically and reported for

0953-8984/90/153529 + 10 $03.50

various systems. Calculated values of L_{in} (1 K) depend on the model and are functions of the film thickness, carrier concentration, the elastic length, the Thomas–Fermi screening length, the density of states at the Fermi energy, the Debye frequency or any of a host of other system parameters. These are sometimes in serious disagreement with the observed values as discussed by White and McLachlan (1989).

The electronic transport properties of disordered bismuth films have been measured by several groups. This work can be separated into two categories. The first category comprises the initial work done on separating out the WAL and associated electron–electron interaction (EEI) components in bismuth, as well as measurements of the magnetoresistance, and in some cases the calculation of parameters such as the elastic and inelastic lengths from the WAL magnetoresistance theories. In this category can be included the work of Komnik *et al* (1981, 1982), Savchenko *et al* (1981), Komori *et al* (1982), Woerlee *et al* (1983), McLachlan (1983) and McLachlan and White (1984). The second (later) category includes far more detailed measurements and analysis of the parameters of the theories, e.g. the inelastic length as a function of temperature. As the characteristics of bismuth films are easily changed in a controllable way by varying the conditions under which the films are deposited, the dependence of the WAL parameters on composition, morphology, thickness, etc, can be studied. Koike *et al* (1985) sputtered bismuth films in the presence of varying partial pressures of oxygen to give granular bismuth–bismuth oxide films covering a large range of resistivities. White (1988) and White and McLachlan (1989) argon ion beam sputtered bismuth films onto glass substrates held at different temperatures. It was found that the substrate temperature during sputtering strongly affected the distribution of crystallite orientations in the films and hence strongly affected parameters such as L_{in}.

In this paper, the effect of varying the carrier concentration on the WAL parameters is studied. As tin is a well known acceptor dopant of bismuth, it is possible to study the dependence of WAL and the associated EEI as a function of carrier type (electron and holes or holes only) and concentration by varying the dopant level. Two methods were utilised to dope the films. The first method involved a uniform dopant distribution obtained by sputtering from an alloyed bismuth–tin target. The second involved a novel method developed by the present authors. Here layered films of Bi–Sn–Bi–Sn . . . were prepared, such that the amount of tin was equal to 1, 2 and 3 at.% (if the tin was homogeneously distributed). From Hall coefficient measurements, the tin in this sandwich configuration was found to dope the bismuth with the number of holes depending on the tin 'concentration'.

It is shown that the temperature coefficient of resistance (TCR) of all the films is negative for $T < 6$ K but that, as the tin concentration is increased from zero to 3 at.%, the TCR (for $T > 6$ K) changes from negative to positive. The origin of a negative TCR in all metallic systems with a high resistivity (the Mooij (1973) criterion) is not at all clear. McLachlan (1982) showed that the sign of the TCR changes from positive to negative when the electron mean free path, the weak-field coherence length and the Fermi wavelength become approximately equal. Tsuei (1986) showed that the sign of the TCR may be interpreted as arising from the interplay between weak localisation and the semi-classical Boltzmann conductivity. Building upon the work of Tsuei (1986), we show in this paper not only that the sign of the TCR is determined by the interplay between WL and the semi-classical conductivity but also that the disorder-induced EEI effects must be included as well. The influence of spin–orbit coupling is also considered.

2. Theory

As a consequence of the high atomic number ($Z = 83$) of bismuth, the resistivity cor-

rections are dominated by spin–orbit scattering. The WAL expressions for the temperature and field dependences of the resistivity, as well as the expressions for the associated EEI temperature dependences will be discussed here for both 2D and 3D. We define $\Delta R(T)/R(T_0) = [R(T) - R(T_0)]/R(T_0)$. In 2D, Hikami *et al* (1980) showed that the correction to the Boltzmann resistivity arising from WAL is given by

$$\Delta R(T)/R(T_0) = (e^2/2\pi^2\hbar)R(T_0)p \ln(T/T_0). \tag{2}$$

Note that the WAL correction gives rise to a positive TCR. Here e is the electronic charge, $\hbar$ is Planck's constant, $R(T)$ is the resistance per unit area. T is the temperature and T_0 is taken to be 4 K.

The correction arising from 3D WAL is given by (Kawabata 1980)

$$\Delta R(T)/R(T_0) = (e^2/2\pi^2\hbar)R(T_0)[T^{p/2}/2L_{in}(1\ K)]. \tag{3}$$

Again it can be seen that the correction arising from WAL in 3D gives rise to a positive TCR. The dimensionality of a film of thickness d is determined by the following criterion:

$$L_{in}(T) > d \qquad \text{for 2D}$$

and

$$L_{in}(T) < d \qquad \text{for 3D}.$$

In the presence of strong spin–orbit scattering, the back-scattering interference which produces WAL is coherent but destructive (Bergmann 1983). Upon application of an external magnetic field, the coherence is destroyed, and hence the magnetoresistance arising from WAL is expected to be positive. The 2D WAL magnetoresistance was calculated by Fukuyama and Hoshino (1981). The magnetoresistance, defined by $\Delta R(B, T)/R(0, T) = [R(B, T) - R(0, T)]/R(0, T)$, is a function of the inelastic length L_{in}, the elastic scattering length L_0 and the spin–orbit scattering length L_{SO}. The respective scattering lengths and times are related by $L_x = (D\tau_x)^{1/2}$.

The positive magnetoresistance arising from WAL in 3D was calculated by Maekawa and Fukuyama (1981). Again, this is a function of L_{in}, L_0 and L_{so}.

The Hall coefficient due to WL was calculated by Fukuyama (1980) and Altshuler *et al* (1980a, b). It was shown that the well known semi-classical expression for the Hall coefficient for a single-carrier system given by

$$R_H = 1/ne \tag{4}$$

remains unchanged in the weak-scattering regime. n is the carrier concentration. The Hall coefficient expression in the two-carrier WAL system is not known to the present authors, but we will postulate that equation (4) remains valid.

Historically, EEIs in disordered media have occupied a somewhat less visible position than WL and WAL. Nevertheless, it is important to realise that the EEI processes are no less important than WL and WAL, and occur in parallel with WL and WAL. Altshuler *et al* (1980a, b) and, independently, Fukuyama (1980) calculated the conductivity arising from the four leading EEI processes. These can be combined to give the 2D EEI correction:

$$\Delta R(T)/R(T_0) = -(e^2/2\pi^2 h)R(T_0)g_{2D}(\text{lo or hi}) \ln(T/T_0). \tag{5}$$

g_{2D}(lo) or g_{2D}(hi) are applicable in zero field or high fields, with the high-field condition determined by $L_B \ll L_T = (\hbar D/kT)^{1/2}$. g_{2D}(lo or hi) is some appropriate combination of the EEI constants g_i ($i = 1, 2, 3, 4$) described by Fukuyama (1983).

As a consequence of the complicated Fermi surface and the possibility of intervalley scattering, coupled with the high spin–orbit interaction strength in polycrystalline bis-

muth-based systems, a precise definition of g_{2D} is not possible, but the value can be estimated from experimental data.

Altshuler *et al* (1980a, b) and Fukuyama (1980) give the EEI expressions in 3D. The temperature dependence of the resistivity is given by

$$\Delta R(T)/R(T_0) = (e^2/2\pi^2 h)R(T_0)g_{3D}(\text{lo or hi})(kT/D\hbar)^{1/2}. \tag{6}$$

Here g_{3D} (lo or hi) is again an appropriate combination of the EEI constants of Fukuyama (1983). The criterion for determining the dimensionality of an EEI system is as follows:

$$L_T = (\hbar D/kT)^{1/2} \begin{cases} > d & \text{for 2D} \\ \text{and} & \\ < d & \text{for 3D.} \end{cases}$$

As regards the EEI contribution to the magnetoresistance, it can be shown that the EEI contribution to the magnetoresistance at 1.5 T is much smaller than the WAL contribution. Furthermore, the multiparameter expressions for the EEI magnetoresistance are particularly complicated, while the 'shape' of the magnetoresistance curves arising from the EEI processes are not markedly different from those arising from WAL. Thus, as the effects are small, and to avoid overparametrisation of the magnetoresistance, the EEI magnetoresistance will be ignored. This is common practice in this field (see, e.g., Bergmann 1984). Therefore the magnetoresistance expressions will not be given in this paper but can be found in the paper of Fukuyama (1983).

Although the EEI contributes to the Hall coefficient as well (Fukuyama 1983), the precise form of the Hall effect in a two-carrier strongly spin–orbit coupled system such as bismuth is not known to the present authors. Hence the Hall coefficient will be interpreted only in terms of the semi-classical result (equation (4)).

3. Experimental results

As disorder is the key feature of the WAL regime, argon ion beam sputtering was used to produce the bismuth-based bilms. The sputtering system has been described in detail elsewhere (White 1988). The sputtering targets were fabricated out of high-purity (99.9999%) bismuth and tin. In the case of the alloyed bismuth–tin targets, the measured amounts of bismuth and tin were melted and mixed under vacuum and then rapidly quenched in cold water. The sputtering targets were mounted on an externally movable target base. Films were sputtered onto glass substrates held at 0 °C. The base pressure in the sputtering chamber was always below 4×10^{-7} mbar before sputtering.

The resistivity, magnetoresistance and Hall coefficient of the sputtered films were measured in a 1.4–273 K cryostat mounted between the poles of a 1.5 T electromagnet. The cryostat has been described in detail elsewhere (White 1988, White and McLachlan 1990).

The temperature of the sample was monitored with a calibrated germanium resistance thermometer below 20 K, and with a calibrated platinum thermometer above 20 K. The resistance, magnetoresistance and Hall coefficient of the sample were measured using conventional bridge and lock-in amplifier techniques via an automated data acquisition–control system, driven by a HP150 computer. The measured data were transferred to an IBM 370 mainframe computer for analysis.

As previously mentioned, two methods were used to dope the bismuth. The first method involved sputtering from targets made up with the required tin concentration. However, chemical analysis showed that the tin concentration in sputtered films was

Table 1. Resistivity, resistance per square, and thickness for all the samples.

Sample	Thickness	ρ ($\mu\Omega$ cm)	$R_\square$ (Ω)
Bismuth–tin (alloyed)	20	1370	687
Bismuth–tin (alloyed)	40	2040	511
Bismuth–tin (alloyed)	100	3170	317
Bismuth–tin (alloyed)	200	3540	117
Bi(10)–Sn(0.48)–Bi(10)	20	670	348
(Bi(4)–Sn(0.03)) × 5	20	1970	985
(Bi(4)–Sn(0.06)) × 5	20	1240	618
(Bi(4)–Sn(0.09)) × 5	20	775	387

always markedly lower than that in the target from which the sputtering was done. The reason for this is not known. Four films of thickness 20, 40, 100 and 200 nm and with a 0.01 at.% tin concentration (as determined from chemical analysis) were sputtered onto substrates held at 0 °C. The TCR (1.4–273 K), magnetoresistance (1.4–15 K) and Hall coefficient (1.4–273 K) of these films was measured. In contrast with pure bismuth (White and McLachlan 1989), the Hall coefficient of these films indicates that the carriers in these systems are predominantly holes. X-ray diffraction indicates that the films are polycrystalline (crystallite diameter, approximately 30 nm) with the distribution of crystallites being very similar to that in pure bismuth films sputtered onto substrates held at 0 °C (White and McLachlan 1989).

The second method involves a novel method of 'doping' developed in our laboratory. 'Sandwich'-type multilayer films were sputtered from separate bismuth and tin targets, with the thicknesses of the respective layers calculated to give the required dopant density. These multilayered films generally consisted of five layers of bismuth layers, 4.0 nm thick, interleaved with tin layers between 0.03 and 0.09 nm (depending on the required dopant density). Note that the thickness of the tin layers is always much less than one monolayer. Hall effect measurements show that the tin apparently acts as an acceptor in these systems, with the hole concentration, as determined from the Hall coefficient, in the Bi(4.0 nm)–Sn(0.03 nm)–Bi(4.0 nm)–Sn(0.03 nm)–Bi(4.0 nm)–Sn(0.03 nm)–Bi(4.0 nm)–Sn(0.03 nm)–Bi(4.0 nm)–Sn(0.03 nm) (abbreviated hereafter as the (Bi(4.0)–Sn(0.03)) × 5 film being a factor of 5 greater than that in a 40 nm 0.01 at.% alloyed film. The carrier concentration in the (Bi4.0–Sn 0.03) × 5 film was calculated to be equivalent to a 0.1 at.% film, and hence (within a factor of 2) this is a gratifying result.

Table 1 gives the resistivities (at 4 K) and thicknesses of all the films. The films sputtered from alloyed targets will be considered first. The magnetoresistance of the films is treated first, as the parameters obtained from these results are used to interpret the TCRs of the films. Finally, the effect of changing carrier concentration on the inelastic length will be considered in terms of existing theories. The magnetoresistance of the films is qualitatively similar to that of pure bismuth films (White and McLachlan 1989) and is shown in figure 1. L_0 was obtained from $E_F\tau_0/h$, with E_F being found in turn from the carrier concentration n obtained from the Hall coefficient. The free-electron model was used in these calculations. The spin–orbit scattering length L_{so} was obtained from the expression of Mersevey and Tedrow (1978) relating the spin–orbit and elastic scattering lengths:

$$(L_{so}/L_0)^2 = 1/(\alpha Z)^4$$

where $\alpha = 1/138$. This relationship holds only to first approximation, as the spin–orbit

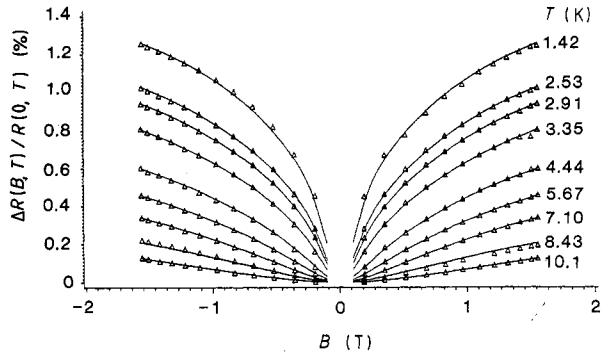

Figure 1. A typical magnetoresistance curve: ———, theoretical fits to the data using equation (4). The temperatures are given to the right of the curves.

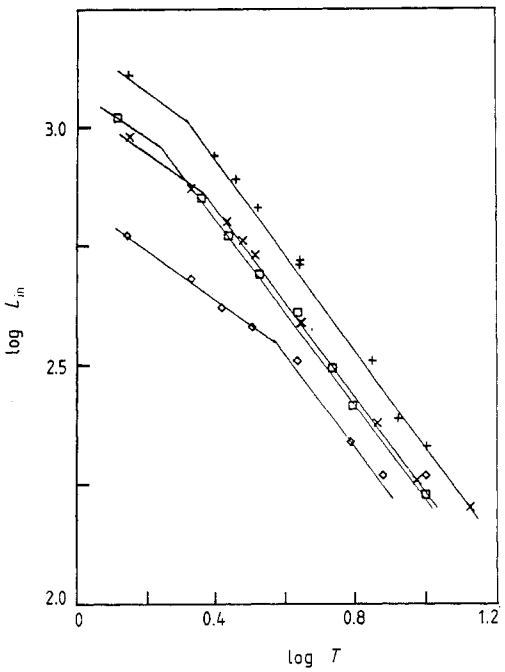

Figure 2. log L_{in} versus log T for the four films sputtered from alloyed targets: +, 20 nm; □, 40 nm; ×, 100 nm; ◇, 200 nm. The slope of the curves give the value of p.

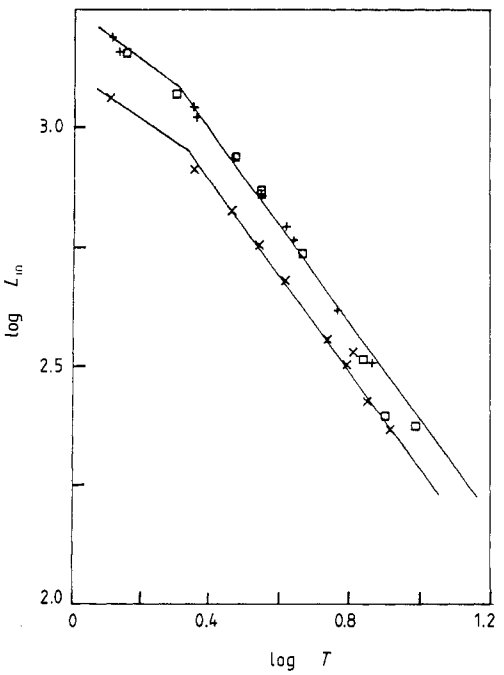

Figure 3. log L_{in} versus log T for the three ten-layer sandwiches: +, 0.03 nm tin layers; □ −0.06 nm tin layers; ×, 0.09 nm tin layers.

scattering may well be enhanced in thinner films, as was found experimentally by Fehr *et al* (1986). Originally L_{SO} was used as an additional fitting parameter as well but, as values of the order of 10 nm were always obtained for all the films, L_{so} was subsequently determined from L_0 and the above equation.

Figure 2 shows the temperature dependence of L_{in} of the alloyed films. As in the case of pure bismuth films sputtered onto substrates held at 0 °C (White and McLachlan 1989), the exponent p of the inelastic length shows a crossover from 1 to 2 at $T \simeq 2.5$ K and $L_{in}(1\text{ K})$ is observed to increase with decreasing film thickness. Note that L_{in} was calculated using the 2D magnetoresistance expression for the 20 and 40 nm films (equation (4)) while L_{in} of the 100 and 200 nm films was calculated from the 3D magnetoresistance expression (equation (6)).

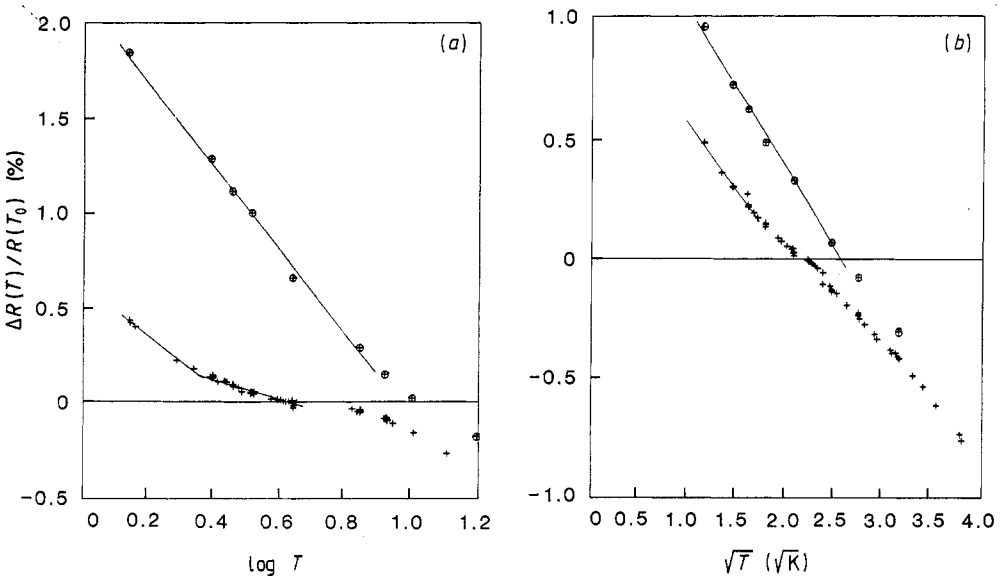

Figure 4. (*a*) Normalised resistivity versus log T for the alloyed 20 nm sample and (*b*) normalised resistivity versus $\sqrt{T}$ for the alloyed 200 nm sample: +, 0 T; ⊕, 1.5 T. p, g(lo) and g(hi) are calculated from the straight-line segments.

As the magnetoresistance of the multilayer films is qualitatively similar to that of the alloyed films, no plots of these results are given. Figure 3 shows the temperature dependence of the inelastic length for the three multilayered 2D films. It can be seen that the value of $L_{in}(1\text{ K})$ is only weakly dependent on carrier concentration. This implies that the strong thickness dependence of the inelastic length in the alloyed film does not originate in the strongly thickness-dependent carrier concentration but is a direct consequence of thickness. A strongly thickness-dependent inelastic length (and carrier concentration) was also observed in pure bismuth films (White and McLachlan 1989) but could not be interpreted because of the more difficult two-carrier nature of pure bismuth.

The TCR data at $B = 0$ T and $B = 1.5$ T can now be interpreted in terms of the magnetoresistance results. Figures 4(*a*) and 4(*b*) show the normalised resistivity of the alloyed 20 and 200 nm films as a function of ln T and $T^{1/2}$, respectively. We can determine g_{2D}(hi) and g_{3D}(hi) from the slope of the $\Delta R(T)/R(T_0)$ versus ln T (for the 20 and 40 nm films) and from the $\Delta R(T)/R(T_0)$ versus $T^{1/2}$ curves (for the 100 and 200 nm films), as WAL is suppressed at 1.5 T. At 0 T, in the 20 and 40 nm films, the slope of the $\Delta R(T)/R(T_0)$ versus ln T curve is proportional to $p - g$(lo) and, since p is known from the magnetoresistance analysis, g(lo) can be determined.

Notice that, since p (in the alloyed films) changes value at $T < 2{\cdot}5$ in all the films, the low-field temperature dependence of $\Delta R(T)/R(T_0)$ is more complicated. Nevertheless, the value of g(lo) for $p = 1$ is similar to that in the $p = 2$ temperature region (within 20–25%). Note that g(lo) cannot be calculated for 3D films because of the combined $T^{1/2}$ EEI and WAL dependences. The situation is further complicated by the presence of the constant D in equation (9) which is effective mass m^* dependent. As a consequence of this, g(hi) for the 100 and 200 nm films is quoted for both holes ($m^* = 0.1m_e$) and electrons ($m^* = m_e$).

$\Delta R(T)/R(T_0)$ for the 2D multilayer films is plotted as a function of ln T in figure 5. As the thickness of the tin layers is increased from 0.03 nm (corresponding to 1 at.% Sn)

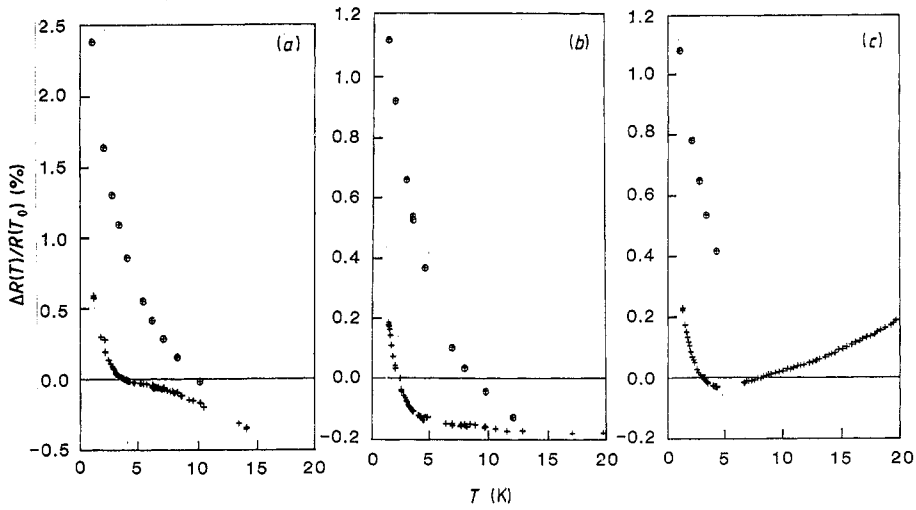

Figure 5. Normalised resistivity versus T for layered films with a tin layer thickness of (a) 0.03 nm, (*b*) 0.06 nm and (*c*) 0.09 nm: +, ○ T; ⊕, 1.5 T.

to 0.09 nm (corresponding to 3 at.% Sn), the TCR (defined as $(1/R)\mathrm{d}R/\mathrm{d}T$) changes from negative to positive for $T \simeq 6$ K. It is our intention to show that this change in the sign of the TCR is a consequence of the delicate interplay between WAL and EEI at different resistivities and carrier concentrations. For combined WAL and EEI in 2D (equations (2) and (8)), the sign of the TCR is determined by the sign of $p - g(\mathrm{lo})$. Since p can be determined from the magnetoresistance analysis, and as we have seen that $g(\mathrm{lo})$ and $g(\mathrm{hi})$ have similar values in the alloyed films and that $g(\mathrm{hi})$ can be determined from the slope of the $\Delta R(T)/R(T_0)$ versus ln T curve, we can thus calculate the approximate value (and hence sign of) $p - g(\mathrm{lo})$ and compare it with the experimentally observed TCR.

A further complication is now apparent: the value of p has been shown to change at $T \simeq 2.5$ K in both alloyed and layered films and now the value of $g(\mathrm{hi})$ also appears to change at around $T \simeq 6$ K; however, the observed changes in both p and $g(\mathrm{hi})$ with increasing temperature are to our advantage, as they permit the value of $p - g(\mathrm{lo})$ to be calculated over three temperature ranges per sample and the resultant sign of $p - g(\mathrm{lo})$ can be compared with the experimental data over all three ranges.

The low-temperature normalised resistivity of the (Bi4.0–Sn0.03) × 5 film as a function of temperature is shown in figure 5(*a*), in both low and high fields. The TCR is negative over the entire measured temperature range. At 1.5 T, the WAL contribution is suppressed, and $g(\mathrm{hi})$ can be determined. From the slope of the curve, we obtain $g(\mathrm{h}) = 1.1$ for $T < 6$ K, and $g(\mathrm{hi}) = 0.7$ for $6\ \mathrm{K} < T < 10$ K. Thus $p - g(\mathrm{lo}) < 0$ for $T < 2.5$ K, but $p - g(\mathrm{lo}) > 0$ for $T > 2.5$ K, in contradiction to the observed sign of the TCR.

The normalised resistivity of the (Bi 4.0–Sn 0.06) × 5 film is plotted as a function of T in figure 5(*b*). The TCR of this film is negative for $T < 30$ K, positive for $30\ \mathrm{K} < T < 80$ K and negative again for $80\ \mathrm{K} < T < 300$ K. Performing a similar analysis to that on the last film gives $g(\mathrm{hi}) = 2.0$ for $1.4\ \mathrm{K} < T < 6$ K, while $g(\mathrm{hi}) = 1.3$ for $6\ \mathrm{K} < T < 10$ K. Here we have $p - g(\mathrm{lo}) < 0$ for $T < 2.1$ K, $p - g(\mathrm{lo}) = 0$ for $2.1\ \mathrm{K} < T < 6$ K, and $p - g(\mathrm{lo}) > 0$ for $6\ \mathrm{K} < T < 10$ K. Again these results are not in agreement with the observed TCR.

Figure 5(*c*) shows the normalised resistivity data for the (Bi 4.0–Sn 0.09) × 5 film. We find that $g(\mathrm{hi}) = 2.7$ for $T < 6$ K, and $g(\mathrm{hi}) = 1.4$ for $T > 6$ K. Hence, if we again assume that $g(\mathrm{lo}) \simeq g(\mathrm{hi})$, then $p - g(lo) < 0$ for $T < 6$ K, and $p - g(\mathrm{lo}) > 0$ for $T > 6$ K, now consistent with the observed experimental data.

The question now arises as to why the calculated values of $p - g(\mathrm{lo})$ are inconsistent with experiment in the (Bi(4.0)–Sn(0.03) × 5 and (Bi(4.0)–Sn(0.06)) × 5 films but are consistent with the data in the (Bi(4.0)–Sn(0.09)) × 5 film. In particular, the prefactors $e^2/2\pi^2h$ are called into question. Note that, if the WAL prefactor had instead been $e^2/4\pi^2h$, or if the EEI prefactor had been e^2/π^2h, then the calculated values of $p - g(\mathrm{lo})$ would be consistent in all three cases.

Other possibilities, such as the increased influence of electron–phonon scattering in less resistive films, are unlikely. This is because the phonon contribution to the resistivity should be independent on disorder but not carrier concentration. In these films, disorder is kept more or less constant, but the carrier concentration is varied. It may thus be concluded that the sign of the TCR might be understood in terms of the delicate interplay between WAL and the associated EEI conductance channels.

4. Conclusions

In this paper we have shown that the low-temperature TCR of our films can be understood directly in terms of the theory (within a factor of 2) and that the use of empirical formulae is not necessary in this case. Furthermore, we have shown that it is necessary to include the effects of the EEI in the work of Tsuei (1986).

Two important questions brought out in this paper, related to the work of Tsuei (1986) and Mooij (1973), are as follows.

(i) Is it possible to find highly resistive films with positive TCR over the whole low-temperature range?

(ii) Can the Mooij (1973) criterion, which is really a room-temperature benchmark, be considered in terms of WL or even a combination of WL and EEI?

References

Abrahams E, Anderson P W, Licciardello D C and Ramakrishnan T V 1979 *Phys. Rev. Lett.* **42** 673
Altshuler B L, Aronov A G and Lee P A 1980a *Phys. Rev. Lett.* **43** 718
Altshuler B L, Khmelnitzkii D E, Larkin A I and Lee P A 1980b *Phys. Rev.* B **22** 5142
Ashcroft N W and Mermin N D 1976 *Solid State Physics* (New York: Holt, Rinehart and Winston)
Bergmann G 1983 *Phys. Rev.* B **28** 515
—— 1984 *Phys. Rep.* **107** 1
Fehr Y, May-tal S and Rosenbaum R 1986 *Phys. Rev.* **33** 6631
Fukuyama H 1980 *J. Phys. Soc. Japan* **48** 2169
—— 1983 *Institute of Solid State Physics, University of Tokyo, Technical Report,* series A, p 1304
Fukuyama H and Hoshino K 1981 *J. Phys. Soc. Japan* **50** 340
Gorkov L P, Larkin A I and Khmelnitzkii D E 1979 *JETP Lett* **30** 228
Hikami S, Larkin A I and Nagaoka Y 1980 *Prog. Theor. Phys.* **63** 707
Kawabata A 1980 *Solid State Commun.* **38** 823
Koike Y, Okamura M and Fukase T 1985 *J. Phys. Soc. Japan* **54** 3018
Komnik Y F, Bukhstaf E I and Nikitin Yu 1981 *Sov. J. Low. Temp. Phys.* **7** 656
Komnik Y F, Bukhstaf E I, Butenko A V and Andrievsky V V 1982 *Solid State Commun.* **44** 865
Komori F, Kobayashi S and Sasaki W 1982 *J. Phys. Soc. Japan.* 51 3136
McLachlan D S 1983 *Phys. Rev.* B **28** 6821
—— 1982 *Solid State Commun.* **42** 521

McLachlan D S and White H 1984 *Proc. Int. Conf. on Localisation, Interaction and Transport Phenomena in Impure Metals* ed L Schweitzer and B Kramer (Braunschweig: Physikalish-Technische Bundesanstalt) p 63
Mersevey R and Tedrow P M 1978 *Phys. Rev. Lett.* **41** 305
Maekawa S and Fukuyama H 1981 *J. Phys. Soc. Japan.* **50** 2516
Mooij J H 1973 *Phys. Status Solidi* a **117** 521
Savchenko A L, Lutskii V N and Rylik A S 1981 *JETP Lett.* **34** 349
Tsuei C C 1986 *Phys. Rev. Lett.* **57** 1943
White H 1988 *PhD thesis* University of the Witwatersrand
White H and McLachlan D S 1989 *J. Phys. C: Solid State Phys.* **1** 6665
—— 1990 *Cryogenics* at press
Woerlee P H, Verkade G C and Jansen A C M 1983 *J. Phys. C: Solid State Phys.* **16** 3011